RSC Advances

PAPER

View Article Online
View Journal | View Issue

Cite this: *RSC Adv.*, 2020, **10**, 1989

Switch on fluorescence mode for determination of L-cysteine with carbon quantum dots and Au nanoparticles as a probe†

Yuye Chen,[a] Xiu Qin,[a] Chunling Yuan[a] and Yilin Wang *[ab]

Citric acid and urea were used as precursors for the preparation of carbon quantum dots (CQDs) which exhibited a maximum emission wavelength at 515 nm when excited at 410 nm. Upon addition of citrate-stabilized Au nanoparticles (AuNPs) with the maximum absorption wavelength at 520 nm, the fluorescence of the CQDs could be efficiently quenched, attributed to the energy transfer between CQDs and AuNPs. However, the further introduction of L-cysteine (Cys) could cause the aggregation of AuNPs along with a drop in absorption at 520 nm, resulting in the fluorescence recovery of the CQDs–AuNPs system. Therefore, a simple and reliable switch on fluorescence sensing platform for determination of Cys was constructed. The significant factors, such as pH and incubation time, that affected the detection of Cys were optimized with the AuNP concentration set as 2.50 nM at room temperature. Under the optimized conditions, the fluorescence recoveries (ΔF) were strongly correlated with Cys concentration in the 0.20 to 4.0 μM range, and the detection limit is 0.012 μM. More importantly, our CQD-based sensing platform was successfully used for the detection of Cys in milk samples with high precision and accuracy, indicating the potential of the probe in practical applications.

Received 1st November 2019
Accepted 5th January 2020

DOI: 10.1039/c9ra09019c

rsc.li/rsc-advances

1. Introduction

As an essential amino acid containing a thiol group, L-cysteine (Cys) is widely used in the pharmaceutical and food industries.[1] It can protect hepatocytes from injury and promote the improvement of liver function.[2] Moreover, as a permitted food additive, Cys is considered to be of both nutritional value and health care function when included in food and nutritional supplements.[3] Therefore, accurate detection of Cys in real samples is very important. So far, various analytical techniques, such as high performance liquid chromatography (HPLC),[4] electrochemistry,[5] colorimetry,[6] fluorescence,[7] *etc.*, have been applied for Cys determination. Among them, a fluorometric method has aroused significant interest owing to the advantages of simple operation, high sensitivity, and fast response. With the development of nanotechnology, some novel fluorescence probes based on nanomaterials have recently been constructed for various analytical applications. For example, Sun's research group[8] provided a switch on fluorescence mode for determining the content of melamine in raw milk using CdS QDs and AuNPs as probe, Yang and coworkers[9] constructed a switch on fluorescent probe composed of carbon quantum dots (CQDs) and AuNPs for highly sensitive measuring organonitrogen pesticide (cartap). A team led by Zhao Jun-Wu[10] reported a method for sensing of Cys using Au–Ag bimetallic nanoclusters (Au–AgNCs) and Au nanorods (AuNRs) as a fluorescence probe. Among the above mentioned switch on fluorescent probes, gold nanomaterials (AuNPs, AuNRs) acted as excellent fluorescence receptors because of their high extinction coefficients and size-dependent absorption spectra. CdS QDs, CQDs and Au–AgNCs served as fluorescence donors. Compared to semiconductors QDs (CdS, CdSe, CdTe) and noble metal nanomaterials (Au–AgNCs), CQDs have advantages of simple preparation, low cost, no toxicity, good biocompatibility, and excellent luminescence properties. According to current literatures, fluorescence assays based on CQDs have been widely used in chemical sensing[11–13] and bioimaging.[14–16] Although the switch on fluorescence probe composed of CQDs and AuNPs has been used for the detection of protamine,[17] melamine,[18] cholesterol[19] and organophosphate pesticides,[20] the fluorescence method based on CQDs and AuNPs for the Cys analysis is rarely reported. We herein demonstrated a fluorescence probe composed of CQDs and AuNPs for switch on detection of Cys, where CQDs as fluorescence reporters and AuNPs as fluorescence quenchers were chosen. The analytical performance of the proposed probe was comparable to or better than those of other reports. It was successfully employed in the detection of Cys in milk samples with high accuracy and good precision.

[a]*School of Chemistry and Chemical Engineering, Guangxi Key Laboratory of Biorefinery, Guangxi University, Nanning 530004, China*

[b]*Guangxi Key Laboratory for Agro-Environment and Agro-Product Safety, Nanning 530004, China. E-mail: theanalyst@163.com; Tel: +86 771 3392879*

† Electronic supplementary information (ESI) available. See DOI: 10.1039/c9ra09019c

2. Experimental section

2.1 Reagents and instruments

Chloroauric acid, L-cysteine (Cys), methionine (Met), cystine (Cyt), histidine (His), lysine (Lys), tryptophan (Trp), threonine (Thr), arginine (Arg), phenylalanine (Phe), valine (Val), alanine (Ala), glycine (Gly), aspartic acid (Asp), lactose and glucose were purchased from Macklin Biochemical Reagent (Shanghai, Co., Ltd., China.). Trisodium citrate dihydrate, citric acid monohydrate, urea, phosphoric acid (H_3PO_4), acetic acid (HAc), boric acid (H_3BO_3), and sodium hydroxide (NaOH) were obtained from Guanghua Sci-Tech Co., Ltd (Guangdong, China.). All reagents in the experiment were utilized without further purification, and doubly deionized water (DDW) was utilized for preparing of all aqueous solutions.

Transmission electron microscopy (TEM) images showing the morphology and size of AuNPs and CQDs were achieved by a Tecnai G2 F20 S-TWIN TEM instrument (FEI Company, America) operating at 200 kV. The zeta potential and particle size distribution was measured by dynamic light scattering (DLS) with a Zeta sizer Nano ZS (Malvern Instruments Ltd., UK). The Fourier transform infrared (FTIR) spectrum of CQDs was obtained with Nicolet iS50 FTIR spectrometer (Thermo, America). The fluorescence spectra of CQDs were recorded on a Shimadzu 5301PC fluorospectrophotometer (Kyoto, Japan), Unico 4802 Ultraviolet-visible spectrophotometer (Shanghai, China) was applied to obtain UV-vis absorption spectra. Measurements of pH were carried out by using a PXSJ-216 acidometer (Shanghai, China) with a combined glass electrode. The centrifugation was performed on an H1850 high speed centrifuge (Changsha, China).

2.2 Preparation of CQDs and AuNPs

The CQDs were prepared according to the literature[21] with some modification. Briefly, citric acid (3.0 g) and urea (3.0 g) were first added into a 100 mL beaker containing 10 mL of DDW to form a clear and transparent solution. Then the beaker had been heated on an electric stove until the solution changed from a colorless liquid to a dark-brown clustered solid. Next, the beaker with solid was moved into an electric vacuum drying oven and had been heated at 60 °C for 1 h. The resulting solution had been centrifuged at 5000 rpm for 20 min, the supernatant was taken and diluted with DDW to 250 mL for further use.

The AuNPs were prepared *via* sodium citrate reduction of chloroauric acid.[20] In a 250 mL beaker, 100 mL of $HAuCl_4$ (1.0 mM) was first heated to boiling under vigorous stirring. 10 mL 1% (w/v) aqueous sodium citrate was quickly poured into the boiled $HAuCl_4$ solution. After the color of above mixture changed from yellow to wine red, boiling was continued for another 15 min. The obtained wine red AuNPs colloid solution was diluted and stored at 4 °C in a refrigerator for further use. The calculated AuNPs concentration was 10 nM according to the absorption and molar extinction coefficient of AuNPs at 520 nm by using Beer's law.

2.3 Procedure for detection of Cys

The CQDs solution was diluted 100 times, and the detection of Cys was performed at room temperature. The CQDs–AuNPs probe solution was first prepared using 1.65 mL of B–R buffer (0.04 M at pH 4.5), 100 μL of CQDs solution and 1.25 mL of AuNPs (10 nM). Various amounts of Cys standard solution were added into the above solution, and then it was diluted to 5.0 mL with DDW. After 25 min, the fluorescence spectra were recorded from 450 to 650 nm with an excitation wavelength of 410 nm (the slit widths of excitation and emission were set at 10 nm and 5 nm, respectively). The calibration curve for Cys was established according to the fluorescence recovery which was defined as $\Delta F = F - F_0$, where F and F_0 denote the emission intensity of CQDs–AuNPs with or without Cys at 515 nm, respectively.

2.4 Milk samples preparation

Two brands of milk were purchased from a supermarket in Nanning, China. The pretreatment procedures of milk were operated according to literature.[22] Briefly, 500 μL of trichloroacetic acid (10%) was doped into the 1.0 mL of milk sample and 250 μL of Na_2CO_3 (1 M) was added to remove protein and calcium. The resulting solution was centrifuged for 10 min at 12 000 rpm, then the supernatant was taken and further filtered through a 0.22 μm membrane. Finally, the samples detection was performed according to the procedure described in Section 2.3.

3. Results and discussion

3.1 Characteristics of CQDs and AuNPs

The morphology and particle size of AuNPs and CQDs were characterized using TEM. As displayed in Fig. 1A, the as-prepared AuNPs are well dispersed and spherical in shape, which are narrow in size distribution and the average diameters are about 13 nm. Fig. 1B indicates that the CQDs are near spherical in shape and uniformly distributed, which are range between 2.4–4.7 nm in diameter (Fig. S1†). The calculated mean particle size was around 3.5 nm, which is in good agreement with that in the literature.[23]

The FTIR is applied to explore the surface groups of the CQDs. As revealed in Fig. 2A, the characteristic absorption bands locating at 3100–3500 cm^{-1} are stretching vibrations of O–H and N–H. The absorption bands at 1600–1700 cm^{-1} are related to the stretching vibration of C=O, and the broad band around 1350–1450 cm^{-1} is ascribed to the bending of C–H.

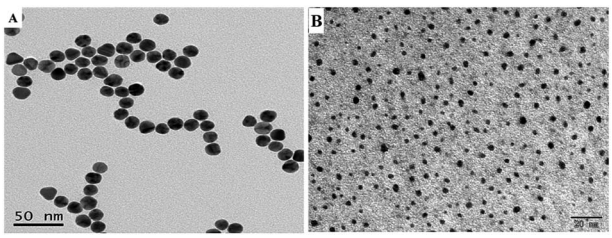

Fig. 1 (A) TEM image of AuNPs. (B) TEM image of CQDs.

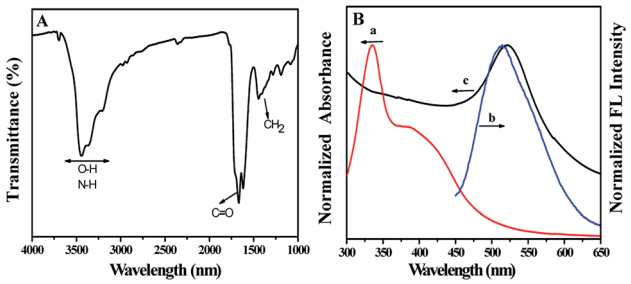

Fig. 2 (A) FTIR spectra of CQDs. (B) Normalized (a) absorption and (b) emission spectra of CQDs, (c) normalized absorption spectra of AuNPs.

These results indicate that carboxyl and amino groups are modified on the surface of CQDs. The existence of carboxyl and amino groups can improve the hydrophilicity and stability of CQDs.

The absorption spectrum of CQDs is wider, and the peak centers locate at 340 nm and 395 nm, respectively, which are the typical absorption of an aromatic π system (curve a in Fig. 2B).[24] And these absorption peaks disclose the hyperconjugation in CQDs structure. Under excited at 410 nm, an emission peak at 515 nm is observed (curve b in Fig. 2B). Fluorescence quantum yield (QY) of CQDs was measured by comparing the wavelength integrated intensity of testing sample to that of quinine sulphate (QY = 54%). According to the calculation method from literature,[25] the QY of as-prepared CQDs was estimated to be 20.8%, which is sufficient for various fluorescence sensing. The as-prepared AuNPs exhibits a strong characteristic absorption peak at 520 nm (curve c in Fig. 2B). Obviously, the emission peak of CQDs is very close to the absorption peak of AuNPs. Thus, if they coexist, the fluorescence of CQDs will be weakened or even quenched by AuNPs.

3.2 The fluorescence quenching of CQDs induced by AuNPs

The influence of AuNPs on the emission spectra of CQDs was studied. As depicted in Fig. 3A, the fluorescence intensity of CQDs decreases with the increase of AuNPs concentration. When AuNPs concentration increases to 2.50 nM, the fluorescence intensity of CQDs is quenched nearly 70%. Previous studies[26,27] have shown that the factors leading to fluorescence quenching are either charge transfer or energy transfer. The former is caused by charge transfer between quencher and fluorophore excited molecules. The occurrence of the latter should satisfy the following conditions at the same time: (1) the emission spectra of donor should be significantly overlapped with the absorption spectra of acceptor; (2) the distance between the acceptor and the donor should be close enough. As mentioned above, the emission spectra of CQDs overlap well with the absorption spectra of AuNPs (Fig. 2B) in present work. The zeta potential measurement of CQDs is +3.67 mV (Fig. S2†), suggesting the CQDs is positively charged. AuNPs is negatively charged with a zeta potential of −33.59 mV, which is consistent with previous report.[17] There is an electrostatic interaction between the positively charged CQDs and negatively charged AuNPs, which can shorten the distance between them and make them close enough. Therefore, we believe that the fluorescence quenching effect of AuNPs on CQDs can be attributed to energy transfer.

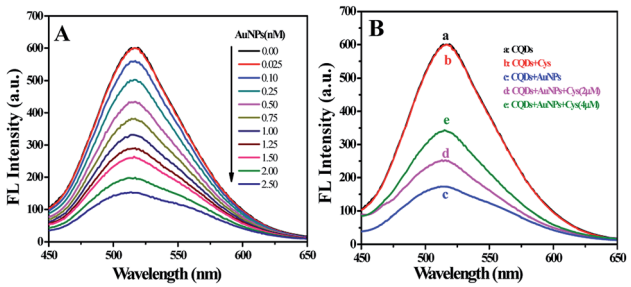

Fig. 3 (A) Fluorescence spectra of CQDs with varying concentrations of AuNPs. (B) Fluorescence spectra of CQDs in different systems.

3.3 The fluorescence recovery of CQDs–AuNPs induced by Cys

The emission spectra of CQDs in different systems were recorded. As displayed in Fig. 3B, the fluorescence spectra of CQDs with and without Cys overlap completely (curve a and b), indicating there is no interaction between them. The fluorescence intensity of CQDs decreases significantly with the appearance of AuNPs (curve c). However, the quenched fluorescence can be recovered with the appearance of Cys (curve d and e). We assume that the fluorescence recovery of CQDs–AuNPs may be the result of the interaction between Cys and AuNPs. To verify this conjecture, the absorption spectra of AuNPs with the presence of Cys at various concentrations were recorded and shown in Fig. S3.† The absorbance of AuNPs at 520 nm decreases while a band located at 650–700 nm appears with the increasing of Cys concentration. Previous researches[28,29] have demonstrated that the surface plasmon absorption of AuNPs is sensitive to the distance between particles. When the distance gets closer, the first peak weakens, and the second red-shifted plasmon absorption peak arises because of the aggregation of AuNPs. As mentioned previously, Cys exhibited a strong affinity for AuNPs, it could be attached onto the surface of AuNPs *via* the sulphur atom of sulfhydryl groups.[29] Owing to OH···N hydrogen bonds between Cys molecules, the Cys-modified AuNPs could be crosslinked to form a three dimensional network, resulting in the aggregation of AuNPs (Fig. S4†). In this work, the aggregation of AuNPs was confirmed by TEM and DLS analysis. The as-prepared AuNPs are well dispersed with

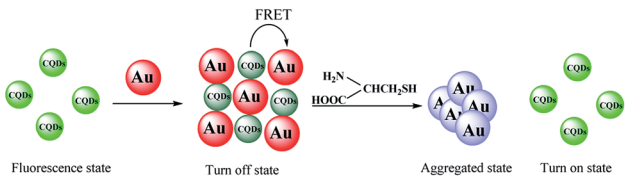

Scheme 1 Schematic diagram of switch on fluorescent mode for Cys assay based on FRET between CQDs and AuNPs.

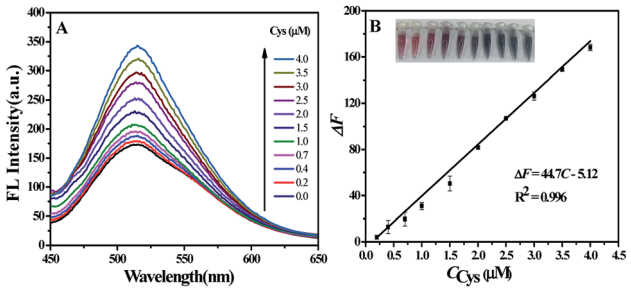

Fig. 4 (A) Fluorescence spectra of CQDs–AuNPs with varying concentrations of Cys. (B) Linear fitting curve of ΔF *vs.* concentration of Cys over a range from 0.20 to 4.0 μM, the inset shows the physical photographs of change in color of CQDs–AuNPs with increased concentrations (from 0.20 to 4.0 μM) of Cys.

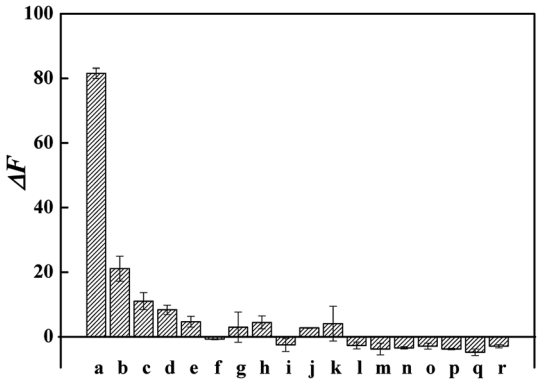

Fig. 5 Fluorescence recovery (ΔF) of CQDs–AuNPs in the presence of Cys and potential interfering substances. Each substance was separately added into CQDs–AuNPs solution in the absence of Cys. From a to r, the corresponding substances are Cys, Met, Cyt, His, Trp, Arg, Lys, Phe, Thr, Val, Ala, Gly, Asp, Ca^{2+}, K^{+}, Mg^{2+}, lactose and glucose.

uniform particle size (Fig. 1A). However, the addition of Cys led to the aggregation of AuNPs (Fig. S5†). As determined by DLS (Fig. S6†), the size distributions of CQDs–AuNPs before and after adding Cys were found in the range of 30–80 nm and 120–180 nm, respectively, indicating the aggregation of AuNPs. In a word, Cys could induce the absorbance decrease of AuNPs at 520 nm, which weakens the energy transfer of AuNPs on CQDs, and then leads to the recovery of the quenched fluorescence emission of CQDs (Scheme 1). Based on the switching effect of Cys on the fluorescence of AuNPs–CQDs system, an effective fluorimetric method can be established for the detection of Cys.

3.4 Detection of Cys with CQDs–AuNPs

In order to achieve the best fluorescence recovery effect, the optimized experiment conditions including pH of buffer, the incubation time and the concentration of AuNPs were performed at room temperature.

pH is an important factor affecting the detection because Cys has various functional groups such as thiol, amine and carbonyl. Hence, the influence of pH was first studied by using B–R buffer with pH value varying from 3.5 to 6.0. As shown in Fig. S7A,† the fluorescence recovery (ΔF) first enhances slowly and then decreases remarkably with the increment of pH value, the maximum ΔF is obtained at pH = 4.5, which was chosen for the further experiments. The effects of incubation time ranging from 5 to 35 min on ΔF were also studied (Fig. S7B†). No significant changes in ΔF are observed after 20 minute incubation. Taken into account the stability of response signal, 25 min was conservatively selected as the optimum incubation time. The low concentration of AuNPs leads to the low degree of fluorescence quenching, which limits the fluorescence recovery and results in a narrow linear range of calibration curve. On the contrary, the linear range of calibration curve becomes wider on the expense of the decrease of sensitivity when the concentration of AuNPs increases. Therefore, the effects of AuNPs concentration varying from 0.5 to 3.0 nM on ΔF were investigated (Fig. S7C†). It was found that the AuNPs concentration had no obvious effect on the ΔF. For consideration of the linear range and the sensitivity, 2.5 nM AuNPs was adopted.

The fluorescence spectra of CQDs–AuNPs with varying concentrations of Cys were recorded. As displayed in Fig. 4A, the fluorescence intensity of CQDs–AuNPs increases with the increase of Cys concentration from 0.2 to 4.0 μM. And the fluorescence recovery (ΔF) is linear to Cys concentration from 0.2 to 4.0 μM (Fig. 4B), the regression equation can be expressed as $\Delta F = 44.7C\,(\mu M) - 5.12$ with a correlation coefficient of 0.996. The limit of detection (LOD) based on $3S_b/k$ for seven measurements of the blank was 0.012 μM. Inset in Fig. 4B is the physical photographs of CQDs–AuNPs with increased Cys concentrations (from 0.20 to 4.0 μM), an obvious color change (from wine-red, purple to blue) is observed with the naked eye. These results suggest that CQDs–AuNPs with two different signals can be employed in the sensitive analysis of Cys.

Table 1 Comparison of present method with other reported Cys fluorescence analysis methods

Probe	Linear range (μM)	LOD (μM)	Response time	References
Au–Ag NCs–AuNRs	5–100	1.73	10 min	10
CL–Cu^{2+}	0–15	0.72	5 s	30
CdTe/CdS QDs–phenanthroline	1.0–70	0.78	55 min	31
Au–Ag NCs	2.0–100	1.1	5 min	32
CQDs–Fe^{3+}	10–200	0.54	Not available	33
CQDs–Rhodamine B–Hg^{2+}	6.0–16.0	0.052	120 s	34
CQDs–AuNCs	1.0–60	0.1	30 min	35
CQDs–AuNPs	0.20–4.0	0.012	25 min	This work

Table 2 Analytical results for Cys monitoring in milk samples ($n = 3$)

Sample	Spiked (μM)	Found (μM)	RSD (%)	Recovery (%)	Found in original sample (μM)
1	0.00	0.81	2.5		162
	0.50	1.28	3.0	94.7	
	0.80	1.58	1.8	96.1	
2	0.00	0.87	3.4		174
	0.50	1.38	1.6	102.3	
	0.80	1.68	3.0	102.0	

A comparison between the developed method with other reported fluorometric methods for Cys analysis are presented in Table 1. It is clear that the LOD obtained by our method is comparable to or lower than those achieved by the other methods. The fluorescence probe used in this work consists of CQDs and AuNPs, which can be prepared under simple conditions, although the linear range of our method here is not the widest. These results indicate that the switch on fluorescence mode based CQDs and AuNPs for Cys assay has high sensitivity.

In order to examine the selectivity of CQDs–AuNPs probe, the fluorescence response of CQDs–AuNPs to Cys, Met, Cyt, His, Trp, Arg (2.0 μM), Lys, Phe, Thr, Val, Ala, Gly, Asp, Ca^{2+}, K^{+}, Mg^{2+}, lactose and glucose (20 μM) were studied according to the procedure described in Section 2.3. ΔF was calculated to assess the selectivity of probe towards Cys. As Fig. 5 displayed, most of these potential interfering substances do not cause any obvious changes in fluorescence signals. However, the presence of Cys, Met, Cyt, and His results in the fluorescence enhancement to some extent on the CQDs–AuNPs probe. The value of ΔF follows the order of Cys > Met > Cyt > His. More importantly, for Met, Cyt, and His, the recovery degree of fluorescence signal is far lower than that for Cys. These experimental results demonstrate that CQDs–AuNPs probe exhibits excellent selectivity to Cys.

3.5 Analysis of milk samples

To further confirm the feasibility of CQDs–AuNPs probe for Cys detection in practical applications, it was used to detect the content of Cys in milk samples. For this purpose, the standard addition method was applied. As can be seen in Table 2, the recoveries were in the range of 94.7–102.3%, and RSDs were less than 5%. The results demonstrate reliability of the probe for acceptable performance in real samples.

4. Conclusions

CQDs were prepared from citric acid and urea, and it was found that the addition of AuNPs results in the fluorescence quenching of CQDs dramatically because of energy transfer. However, the further introduction of Cys could cause the aggregation of AuNPs, resulting in the fluorescence recovery of CQDs–AuNPs system. A simple and fast detection method based on CQDs–AuNPs as a fluorescent probe was developed for selective detection of Cys. The analytical performance of the proposed probe was comparable to or better than those of other reports. The advantages of the method are simplicity, low-cost, high accuracy and good precision.

Conflicts of interest

The authors declare that they have no competing interests.

Acknowledgements

The authors thank the National Natural Science Foundation of China (21567002), the Opening Project of Guangxi Key Laboratory for Agro-Environment and Agro-Product Safety (17-259-82) and the Dean Project of Guangxi Key Laboratory of Biorefinery (201801) for their financial support.

References

1 Y. Chen, T. Chen, X. Wu and G. Yang, *Sens. Actuators, B*, 2019, **279**, 374–384.
2 M. Lin, Y. Guo, Z. Liang, X. Zhao, J. Chen and Y. Wang, *Microchem. J.*, 2019, **147**, 319–323.
3 J. Wang, H. Wang, Y. Hao, S. Yang, H. Tian, B. Sun and Y. Liu, *Food Chem.*, 2018, **262**, 67–71.
4 Q. Xiao, H. Gao, Q. Yuan, C. Lu and J. M. Lin, *J. Chromatogr. A*, 2013, **1274**, 145–150.
5 S. Yang, G. Li, C. Qu, G. Wang and D. Wang, *RSC Adv.*, 2017, **7**, 35004–35011.
6 Y. Wang, S. Tang, H. Yang and H. Song, *Talanta*, 2016, **146**, 71–74.
7 Y. Mao, C. Zhao, S. Ge, T. Luo, J. Chen, J. Liu, F. Xi and J. Liu, *RSC Adv.*, 2019, **9**, 32977–32983.
8 X. Cao, S. Fei, M. Zhang, J. Guo, Y. Luo, L. I. Xing, L. Han, C. Sun and J. Liu, *Food Control*, 2013, **34**, 221–229.
9 Y. Yang, J. Hou, D. Huo, X. Wang, J. Li, G. Xu, M. Bian, Q. He, C. Hou and M. Yang, *Microchim. Acta*, 2019, **186**, 259.
10 J. Li, D. Qiao, J. Zhao, G. J. Weng, J. Zhu and J. W. Zhao, *Spectrochim. Acta, Part A*, 2019, **217**, 247–255.
11 A. M. Su, D. Wang, X. Shu, Q. M. Zhong, Y. R. Chen, J. C. Liu and Y. L. Wang, *Chem. Res. Chin. Univ.*, 2018, **34**, 164–168.
12 X. Zhao, S. Liao, L. Wang, Q. Liu and X. Chen, *Talanta*, 2019, **201**, 1–8.
13 Y. Che, H. Pang, H. Li, L. Yang, X. Fu, S. Liu, L. Ding and J. Hou, *Talanta*, 2019, **196**, 442–448.
14 H. Li, F. Q. Shao, H. Huang, J. J. Feng and A. J. Wang, *Sens. Actuators, B*, 2016, **226**, 506–511.

15 W. J. Niu, Y. Li, R. H. Zhu, D. Shan, Y. R. Fan and X. J. Zhang, *Sens. Actuators, B*, 2015, **218**, 229–236.
16 X. Yang, Y. Wang, X. Shen, C. Su, J. Yang, M. Piao, F. Jia, G. Gao, L. Zhang and Q. Lin, *J. Colloid Interface Sci.*, 2017, **492**, 1–7.
17 H. Rao, H. Ge, X. Wang, Z. Zhang, X. Liu, Y. Yang, Y. Liu, W. Liu, P. Zou and Y. Wang, *Microchim. Acta*, 2017, **184**, 3017–3025.
18 H. Dai, Y. Shi, Y. Wang, Y. Sun, J. Hu, P. Ni and Z. Li, *Sens. Actuators, B*, 2014, **202**, 201–208.
19 Y. Li, J. Cai, F. Liu, H. Yang, Y. Lin, S. Li, X. Huang and L. Lin, *Talanta*, 2019, **201**, 82–89.
20 X. Wu, Y. Song, X. Yan, C. Zhu, Y. Ma, D. Du and Y. Lin, *Biosens. Bioelectron.*, 2017, **94**, 292–297.
21 S. Qu, X. Wang, Q. Lu, X. Liu and L. Wang, *Angew. Chem.*, 2012, **51**, 12215–12218.
22 X. Chen, W. Ha and Y. P. Shi, *Talanta*, 2019, **194**, 475–484.
23 X. Li, Y. Zheng, Y. Tang, Q. Chen and Q. Wang, *Spectrochim. Acta, Part A*, 2018, **206**, 240–245.
24 A. Kumar, A. R. Chowdhuri, D. Laha, T. K. Mahto, P. Karmakar and S. K. Sahu, *Sens. Actuators, B*, 2017, **242**, 679–686.
25 S. Chandra, V. K. Singh, P. K. Yadav, D. Bano, V. Kumar, V. K. Pandey, M. Talat and S. H. Hasan, *Anal. Chim. Acta*, 2019, **1054**, 145–156.
26 A. Su, Q. Zhong, Y. Chen and Y. Wang, *Anal. Chim. Acta*, 2018, **1023**, 115–120.
27 J. S. Sidhu, A. Singh, N. Garg, N. Kaur and N. Singh, *Sens. Actuators, B*, 2019, **282**, 515–522.
28 Y. Zhang, J. Jiang, M. Li, P. Gao, Y. Zhou, G. Zhang, S. Shuang and C. Dong, *Talanta*, 2016, **161**, 520–527.
29 N. Gao, P. Huang and F. Wu, *Spectrochim. Acta, Part A*, 2018, **192**, 174–180.
30 Q. Meng, H. Jia, P. Succar, L. Zhao, R. Zhang, C. Duan and Z. Zhang, *Biosens. Bioelectron.*, 2015, **74**, 461–468.
31 S. Chen, J. Tian, Y. Jiang, Y. Zhao, J. Zhang and S. Zhao, *Anal. Chim. Acta*, 2013, **787**, 181–188.
32 T. Feng, Y. Chen, B. Feng, J. Yan and J. Di, *Spectrochim. Acta, Part A*, 2019, **206**, 97–103.
33 H. Wu, J. Jiang, X. Gu and C. Tong, *Microchim. Acta*, 2017, **184**, 2291–2298.
34 Y. Liang, Q. Zhao, X. Wu, Z. Li, Y. J. Lu, Q. Liu, L. Dong and C. Shan, *J. Alloys Compd.*, 2019, **788**, 615–622.
35 X. Yu, C. Zhang, L. Zhang, Y. Xue, H. Li and Y. Wu, *Sens. Actuators, B*, 2018, **263**, 327–335.